ECCOMAS Congress 2016
VII European Congress on Computational Methods in Applied Sciences and Engineering
M. Papadrakakis, V. Papadopoulos, G. Stefanou, V. Plevris (eds.)
Crete Island, Greece, 5–10 June 2016

SEISMIC BEHAVIOR INDICES OF OLD TYPE REINFORCED CONCRETE MEMBERS

Anthos I. Ioannou [1], Stavroula J.Pantazopoulou

[1] University of Cyprus Department of Civil and Environmental Engineering P.O. Box 20537, 1687 Nicosia, Cyprus
e-mail: ioannou.anthos@ucy.ac.cy

Keywords: shear-strength models, shear failure, axial load, drift ratio models.

Abstract. *The study reviews the existing methods for estimation of the peak and residual shear strength of columns and the main parameters that affect their shear drift capacity. Shear force effects on the behavior of the columns seem to be significant as shear influences the flexural behavior of columns and encourages failure mechanisms that are more brittle, especially for columns which are shear critical (columns over-reinforced in flexure, short columns). The methods that have been developed up until now for the estimation of shear strength vary, but in all cases contributions from separate mechanisms of resistance, namely the contribution of concrete, web reinforcement and axial load are recognized. In establishing the degradation of shear strength under seismic load reversals the decomposition of concrete cover, the diagonal strut cracking of the element and the yielding or slip of the longitudinal reinforcement are determined. Another important parameter which must be taken into account in experimental results for the calibration of previous methods in establishing the rate of strength degradation as well as the residual strength is the contribution of axial load to the load-carrying capacity loss, with increasing displacement. This phenomenon is shown to be significant and for that reason separation from the other mechanisms of degradation will be essential in revision and refinement of design expressions for shear, necessary in assessment procedures. An analytical investigation of the relationship between shear drift capacity, transverse reinforcement, aspect ratio and axial load is presented in the paper.*

Introduction

Condition assessment of an existing reinforced concrete structure is the first step towards retrofit design and strengthening. Reinforced Concrete (R.C.) columns represent the most critical components in this assessment problem, as their possible failure can place at risk the integrity of the structure and its ability to support gravity loads. Thus, dependable assessment of columns is a prerequisite for the successful redesign of a structure, and requires a good understanding and interpretation of the current condition. A critical part of this procedure is the estimation of the degraded shear strength of reinforced concrete columns after inelastic reserved cyclic displacements such as those occurring during a severe earthquake. In the context of the following investigation, performance assessment makes direct reference to the state of damage attained by the examined member. Damage is quantified in terms of lateral drift ratio. To facilitate calculations at distinct performance limits, drift capacity is estimated at the point of shear and axial failure on the experimental envelope curve. Current methods used in design codes to estimate the extent of degradation of shear strength with increasing displacement demand are built on previous researches by Aschheim(1992), Lynn(2001), Sezen(2002) and Elwood(2003). However, collective evaluation of the available data identify that certain parameters may have a great than what was thought before effect on the overall mechanism of shear strength degradation and on the deformation capacity of the member at performance limit states; such are, the aspect ratio, the second order effects generated by axial load, and the effect of transverse reinforcement ratio on the value of drift at failure. For this reason this problem is revisited aiming for a better understanding of the relationship between shear strength, P-Δ effects, and the drift ratios at shear and axial load failure.

In particular, evaluation of the residual shear strength of a member after degradation due to excessive displacement has set-in is a focal point of this study. While the displacement increases well beyond the peak point of the resistance curve of the member, the load-carrying capacity decreases owing to a variety of reasons, several of those reflecting implicit shear failure, such as diagonal tension cracking in the web of the member, yielding of longitudinal reinforcement, excessive compressive strains in the compression zone, loss of bond strength of the longitudinal reinforcement and disintegration of the web concrete due to diagonal compression. In some situations other effects may be responsible for what is often interpreted as damage-induced strength degradation – this refers to the influence of second order effects imparted by the axial load while the deformation increases. Especially this phenomenon seems to contribute dramatically to the macroscopically observed loss of lateral resistance, and the confusions caused thereof is occasionally passed-on into the calibrated expressions for shear-strength assessment of columns (the k(μ) factor, see ASCE/SEI 41, 2007). Linked with this is the value of drift at the onset of shear and axial failure. To address this problem from the beginning, a data base of 135 old type R/C columns has been created and an algorithm is followed taking into consideration the second order effects in correcting the experimental resistance envelope curves for some of the specimens. Comparison between the existing calibrated models for the evaluation of shear strength and the results illustrates the significance of second order effects on shear strength degradation. Experimental values of shear and axial drift ratios at the corresponding limit states are compared with values obtained from the proposed models. An investigation of how the values of aspect ratio, transverse reinforcement ratio and axial load influence the values of drift ratio at the reference limit states is also included in the discussion.

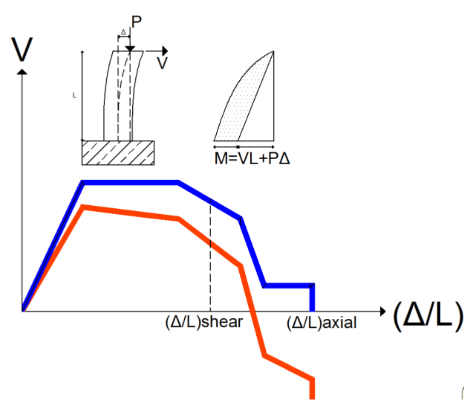

Figure 1 Schematic representation of the effects of P-Δ on the response curve of a member. Vertical axis represents the shear force required to produce a given drift magnitude (horizontal axis coordinate) if axial load is not considered (blue line) and after correction for the P- Δ effects (red line).

1 SHEAR STRENGTH

To investigate the behavior of columns under seismic shear, a data base of column tests was assembled. The data base contains columns of different cross sectional shapes, and tested under cyclic loading in single and double curvature simulating the action of earthquakes. Most of the specimens were observed to exhibit shear failure. Additionally, a small number of spiral columns were selected for study that failed in flexure. Important response parameters selected for the data base were the drift ratios at shear and axial failure, depicted in Fig. 1, and denoted as $(\Delta/L)_{shear}$ and $(\Delta/L)_{axial}$, respectively. According to the established practice in the field, the drift at shear failure is identified as the point where a 20% loss in lateral load carrying capacity is observed, whereas the drift at axial failure is associated with loss of axial load carrying capacity – i.e. collapse (this point sometimes may be identified as the final point of the envelope curve). Parameters used in the investigation were the following: the aspect ratio M/(Vd), the transverse reinforcement ratio ρ'', the average axial load ratio, $v_d=P/A_g f_c'$, the longitudinal reinforcement ratio and the material properties of the specimens. Values of the parameters for all assembled specimens are illustrated in the Table 4 in Appendix A . The specimens are categorized according to cross-section shape.

- Rectangular shaped columns
- Circular shaped columns
- L shaped columns.

The nominal shear strength of a reinforced concrete member, V_n , is estimated from the contribution of various strength components, namely, a contribution of the concrete web, V_C (comprising shear transfer over the compression zone, aggregate interlock and dowel action over the tension zone) and the contribution of transverse (web) reinforcement V_s as illustrated in Figure 3 (Elwood et al 2003). In most cases of design guidelines around the world the contribution of axial load, is either considered separately, or it is embedded in V_C.

$$V_n = V_C + V_s \tag{1}$$

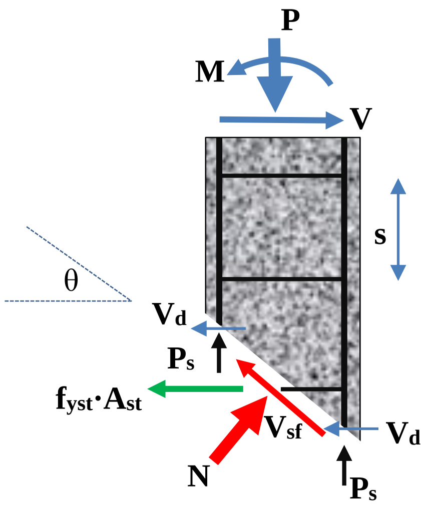

Figure 2 Components of shear force across a diagonal crack near failure (from Elwood 2003).

Because shear failure is a brittle mode of failure it is generally placed higher in the strength hierarchy scheme of capacity design, as compared to flexural failures; in the strength inequality flexural strength defines the demand for shear design of new, or the basis of assessment in existing members. As it is desirable to maintain shear demand below shear strength at least within the range of design displacements (i.e. up to a displacement ductility of 5), strength is estimated by considering all possible forms of disintegration that may limit its magnitude. Strength reduction is effected by multiplying the nominal strength by a multiplier that accounts for the various effects that are responsible for shear strength loss, originally proposed by Aschheim and Moehle (1992) and later refined by several other researchers. Available proposals to date are listed in the table below:

Researcher	**Shear Strength Proposed Models**
Aschheim (1992), 45° truss angle corresponding to the approximate initial angle typically assumed by shear cracks	$V = V_C + V_s; \quad V_C = a'(1+\frac{N_u}{2000A_g})\sqrt{f_c}bd \le 3.5\sqrt{f_c}bd$ For rectangular columns : $V_s = A_v f_{y,tr} d/s$ For spiral columns : $V_s = 2A_{sp} f_{y,tr}(0.8d_s)/s$
Lynn and Moehle (2001), 45° truss angle in this proposal. $\mu_\delta \le 1$ k=1 $1 \le \mu_\delta \le 6$ k varies from 1 and 0.7 $\mu_\delta \ge 6$ k=0.7	$V_n = kV_c + \frac{1}{2}V_c = k\frac{A_g 0.5\sqrt{f_c}}{\frac{a}{d}}\sqrt{1+\frac{P}{0.5A_g\sqrt{f_c}}} + \frac{1}{2}\frac{A_{s,tr} f_{y,tr} d}{s}$
Sezen and Moehle (2002), 45° truss (based on calibration of tests, the average truss angle is found near 55°). Parameter *k* ranges between 1.0 and 0.7 based on average shear crack angle for the test columns in the database (55°) and 45° crack angle, respectively.	$V_n = k(V_c+V_s) = k\frac{A_{s,tr} f_{y,tr} d}{s} + k\left(\frac{0.5\sqrt{f_c}}{\frac{a}{d}}\sqrt{1+\frac{P}{0.5A_g\sqrt{f_c}}}\right)0.80A_g$
Elwood and Moehle (2003), At shear failure (stirrup yielding) the truss angle is equal to **65°** or may be better approximated by θ=55°+35°· (P/P$_o$)	$V = \frac{A_{s,tr} f_{y,tr} d_c}{s}\tan\theta - P\left(\frac{25\frac{\Delta}{L}}{1+\tan^2 - \tan\theta\frac{\Delta}{L}}\right)$
Dionysis E. Biskinis, George K. Roupakias, and Michael N. Fardis(2004): from calibration of extensive database of tests. Mean values considered, $\gamma_V=1$	$V_R = \gamma_V \cdot \left[\frac{b-c}{2L_s}min(N;0.55A_c f_c) + (1-0.55,min(5;\mu_\Delta^{pl}))\right.$ $\left.\left[(0.16\,max(0.5;100\rho_{tot})(1-0.16,min(5,\frac{L_s}{b}))\sqrt{f_c}A_c + V_s\right]\right]$
EC8 Part III: same as above, with $\gamma_V=0.85$	
ASCE/SEI 41 k = 1 for μ ≤ 2 k= 0.7 for μ≥6 k varies linearly for 2<μ<6 λ= 0.75 for LWA concrete and 1.0 for NWA concrete.	$V_n = k\frac{A_v f_y d}{s} + \lambda k\left(\frac{0.5\sqrt{f_c}}{M/Vd}\sqrt{1+\left(\frac{N_u}{6\sqrt{f_c}A_g}\right)}\right)0.8A_g$

Table 1 Proposed Models for the evaluation of the degraded shear strength.

Notation: L=length of the column; b=column section width; h=column section height; d=depth to centerline of tension reinforcement; a= shear span; s=tie spacing; ρ_l*=longitudinal reinforcement ratio (*$A_{st}/(b_s)$*),* ρ''*=transverse reinforcement ratio (*$A_{st}/(bs)$*);* f_{yl}*=longitudinal steel yield strength;* f_{yt}*=transverse steel yield strength ;* f_c' *=concrete strength;* $P/(A_g{*}f_c')$*= constant axial load; (M/(Vd))=aspect ratio; Δ/L=drift; c=neutral axis depth;* A_c*=web cross sectional area;* μ_Δ^{pl}=plastic part of ductility demand; ρ_{tot}=total longitudinal reinforcement ratio; V_s=contribution of transverse steel; V_C=concrete web contribution

As is shown in Table 1, the shear strength models include coefficients that estimate the reduced shear strength. The strength reduction is attributed to the degradation of the concrete web which carries the shear through diagonal compressive struts. However, shear force measured in columns while conducting tests to lateral displacement (drift) history, undergoes an apparent loss of magnitude with increasing displacement, even if no web damage could be detected (e.g. in flexural response), and this is due to the second order effects of the column axial load as the longitudinal axis of the member is displaced from the reference point. This apparent reduction of column strength, *dV*, may calculated after consideration of the column in the deformed configuration. Thus, to maintain constant flexural moment at the column base, M_o, the shear force $V(\Delta)$ may be estimated from: $V(\Delta) = (M_o - P\cdot\Delta)/L = V_o - (P\cdot\Delta/L)$, thus $dV = -P\cdot\Delta/L$. Today with the vast number of available column experiments it appears that strength degradation may be overestimated, or may be insensitive to some important relevant parameters. Although behavioral factors such as diagonal cracking of concrete (flexural yielding, splicing of reinforcement in critical regions, compression buckling of longitudinal reinforcement) are the prime culprits, there is no question that second order effects consume a large fraction of the available strength giving the impression that strength loss takes place. It is actually a debated question whether the experiments used to calibrate the expressions for the degradation coefficient were corrected for *dV* before estimating the real strength loss with increasing displacement (Fardis et al.(2004), EC8, ASCE/SEI 41, Elwood and Moehle (2003), Sezen and Moehle (2002), Lynn and Moehle (2001) and Aschheim and Moehle (1992)).

In this paper this problem is revisited by studying strength loss only once after the data were systematically corrected in a uniform manner for the second order effects. The methodology followed in this process is described in detail: In order to understand the degree of influence of second order effects on shear strength, the experimental results will be compared with the results obtained from the proposed models as described in Table 1. As a first step the resistance curve was evaluated for each specimen contained in the database using established sectional analysis software (Response-2000). Next the analytical resistance envelope curve is analyzed and corrected accounting for second order effects; the corrected curve is subsequently compared with the experimental resistance envelope. Any residual difference observed between the experimental curve and the analytical curve after correction for P-Δ may be attributed to other sources of degradation such as compression softening of concrete and disintegration of the web of the member. See the figure below:

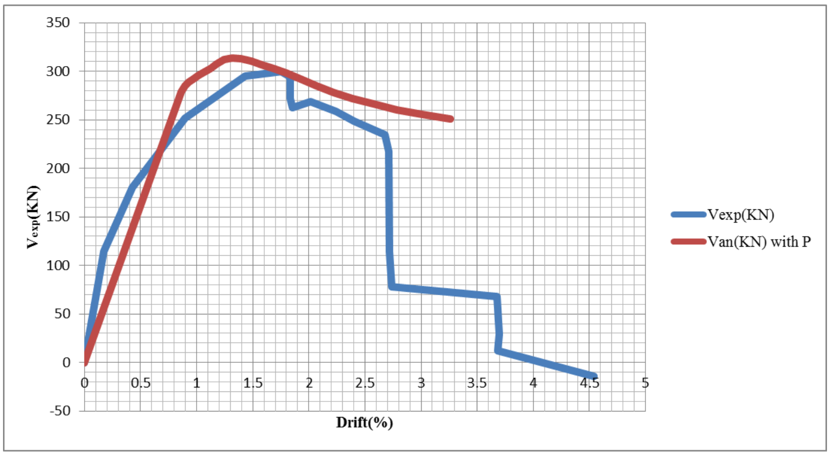

Figure 3 Comparison of the analytical envelope curve after considering the second order effects with the experimental envelope curve.

The background concept of this procedure is as follows: Ideally, a reinforced concrete member that undergoes flexural yielding without any shear degradation, would exhibit a response curve that is either elastoplastic or elastoplastic with hardening. Deviation from this ideal response may be owing to both, disintegration and P-Δ effects. Both of these components increase with deflection, however the latter of the two terms is easy to calculate given the lateral displacement of the column and the shear span length, L_s. The objective is therefore, to separate the contributions of these two sources of apparent strength loss by restructuring the total deviation of the actual response curve from its undegraded flexural response curve. Thus, the total lateral force reduction, ΔV comprises components as:

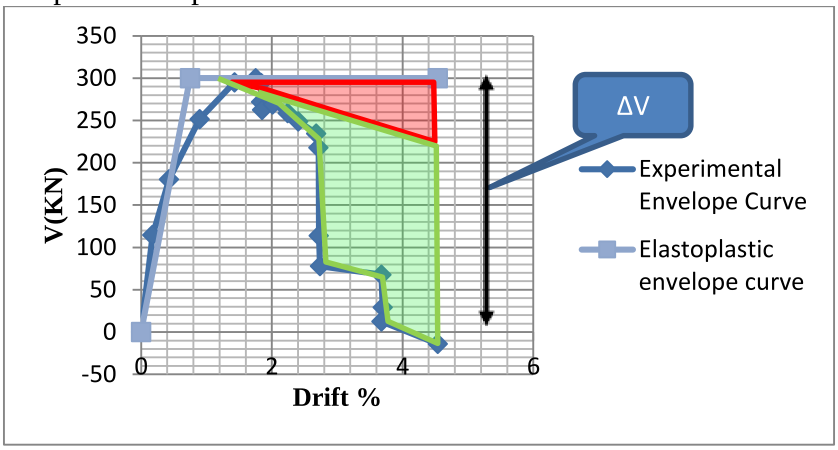

Figure 4 Difference between the elastoplastic and the experimental envelope curve. Red is the load carrying capacity occupied by P-Δ; Green is the load carrying capacity degraded (non-recoverable) due to damage.

$$\Delta V = \Delta V_{red} + \left(\frac{P\Delta}{L_s}\right) \Rightarrow \Delta V_{red} = \Delta V - \left(\frac{P\Delta}{L_s}\right) \tag{2}$$

ΔV= the difference between the elastoplastic and the experimental envelope curve
P= the axial load
Δ= the horizontal displacement
L_s = the span length of the column between the fixed support and the point of zero moment.

Therefore, a relationship is sought between the corrected shear strength degradation term, ΔV_{red}, and the drift ductility μ_θ. Figures 10 in Appendix B illustrates the graph obtained from the experimental results and the results exported from Equation 2. Figure 11 in Appendix B illustrates the comparison between $\Delta V_{red}/V_{max}$, $\Delta V/V_{max}$ with the results for normalized strength degradation as obtained from the available shear strength degradation models proposed by, Aschheim and Moehle (1992), Elwood and Moehle (2003), and Sezen and Moehle (2002). Calculation of ΔV estimated by each of the models was done according to the following procedure:

(1) Calculation of $V_{shear,max}$ for the minimum value of μ_n (ductility).
(2) For the minimum value of drift ductility μ_1 it turns out the following relationship : $V_1 = V_{\max} \Rightarrow$ for μ_{v+1} is applicable $V_{n+1} \le V_{\max}$
(3)Then $\Delta V = \left(\frac{V_{\max} - V_{n+1}}{V_{\max}}\right)$

2 SHEAR AND AXIAL DRIFT CAPACITY

Another aspect in the evaluation procedure is deformation capacity. It is established in the literature to refer to deformation capacity at the onset of shear and axial failure. Expressions have been proposed to that effect (Elwood and Moehle, 2003); these were used and the analytical results were compared with the experimental values. Expressions are obtained after empirical evaluation of the experimental database assembled by the investigators. Note that it is possible that this model may not be appropriate (applicable) for columns that were not included in the author's Database, as most of the specimens used to calibrate the expressions for the milestone drift capacities only come from a single research team. The aim of the present investigation is to calculate this shear drift capacity model for different types of columns and to observe the results.

The function used by Elwood and Moehle (2003) to estimate the drift ratio at shear failure of a column under lateral sway is as follows:

$$\left(\frac{\Delta_s}{L}\right)=\frac{3}{100}+4\rho_t-\frac{1}{500}\frac{v}{\sqrt{f_c}}-\frac{1}{40}\frac{P}{A_g f_c}\geq\frac{1}{100} \quad \text{(in psi units)} \tag{3}$$

A comparison between the experimental and analytical results obtained for the shear drift capacity was conducted. The experimental shear force is compared with the value of shear force obtained from Response 2000 analysis taking into account the influence of second order effects and the aspect ratio of the member considered. A parametric investigation between transverse reinforcement ratio, axial load ratio, aspect ratio and experimental shear drift values was conducted.

Another concern is the estimation of the drift ratio at column axial failure. This is an extreme stage where the column is near imminent collapse. At this stage it is assumed that whatever residual shear strength is available to the column, this is owing to the frictional resistance that develops along the failure plane which is inclined at an angle θ from the member cross section (Fig. 2, see term V_{sf}). Based on this frictional concept,

$$V_{sf}=N\mu \tag{3}$$

The equations representing equilibrium of forces along x and y of the Free-Body Diagram of the column model depicted in Fig. 2 are as follows:

$$\Sigma F\chi\rightarrow \mathrm{N}\sin\theta+V=V_{sf}\cos\theta+\frac{\mathrm{A}_{st}f_{yt}d_c}{s}\tan\theta \tag{4}$$

$$\Sigma Fy\rightarrow P=N\cos\theta+V_{sf}\sin\theta+n_{bar}P_s \tag{5}$$

Since imminent collapse is considered, the external shear resisted, V is now taken equal to zero. Thus, Equation (3) will take the following form:

$$\Sigma F\chi \rightarrow N\, sin\,\theta = N \cdot \mu\, cos\,\theta + \frac{A_{st} f_{yt} d_c}{s} tan\,\theta, \quad \text{and,} \quad \Sigma Fy \rightarrow P = N(cos\,\theta + \mu\, sin\,\theta) + n_{bar} A_b f_y \tag{6}$$

The coefficient of friction and the angle θ of the failure plane are required to perform a calculation; Elwood and Moehle (2003) using the results from their own database and using constant value of shear angle $\theta = 65^o$ calculated the coefficient of friction. As a result of this investigation proposed the following relationship between the effective coefficient of friction and the drift ratio at axial failure for the total capacity model.

$$\mu_t = \tan\theta - \frac{100}{3}\left(\frac{\Delta}{L}\right)_{axial} \geq 0 \tag{7}$$

Furthermore the coefficient of friction μ can be calculated from the following equation:

$$\mu = \frac{V}{N} \tag{8}$$

Calibration between the two equations, i.e., (7) and (8) is used to obtain the following expression for the drift at axial failure.

$$\left(\frac{\Delta_a}{L}\right) = \frac{0.5}{5 + \dfrac{Ps}{A_{tr} f_{yt} d_c}} \tag{9}$$

According to Elwood and Moehle (2003), the precision of such a model is comparable to that for the strength, since the longitudinal reinforcement capacity is not controlled when the drift ratios in the tests are recorded. The model requires information only about the transverse reinforcement and the axial load. In the present study a comparison is carried out between the results from Equation (9) and the independently assembled database of tests, presented herein. A next step investigating the performance of the proposed relationship for the axial drift ratio at failure is the parametric analysis of the effect of aspect ratio, taking into account the transverse reinforcement ratio and the axial load ratio considering collectively all the tests of the database.

4.0 DISCUSSION OF INVESTIGATION RESULTS

To investigate the influence of second order effects on shear strength degradation a bar chart was prepared to check the results for eight selected column specimens obtained from the data base. The specimens are shown in Table 2 and all the geometrical and mechanical properties can be found in Table 4 of Appendix A.The criterion of specimens selection was the same value of displacements ductility μ=4 due to the fact that for high values of displacements, the contribution to shear strength degradation is bigger.Figure 5 compares for a displacement ductility of μ=4 the ratios $\Delta V/V_{max}$, $\Delta V_{red}/V_{max}$ with the corresponding values which are obtained from the shear strength models of Table 1. According with the procedure described in section 2, and as shown in Figure 5, shear strength is decreased with increasing displacement ductility. More specifically, it may be seen in Fig. 8 which compares the ratios $\Delta V/V_{max}$ and $\Delta V_{red}/V_{max}$

for each specimen that a lower strength degradation occurs than previously thought, when the second order effects are accounted for; at the same time, the total strength loss expressed by the *$\Delta V/V_{max}$* ratio is underestimated. The first of the models (Ashheim and Moehle 1992) is particularly unconservative. Overall, the model by Elwood and Moehle (2003) gives the closest approximation to the experimental results, although it appears that this too requires improvement (Fig. 8, Table 2) to better match the tests.

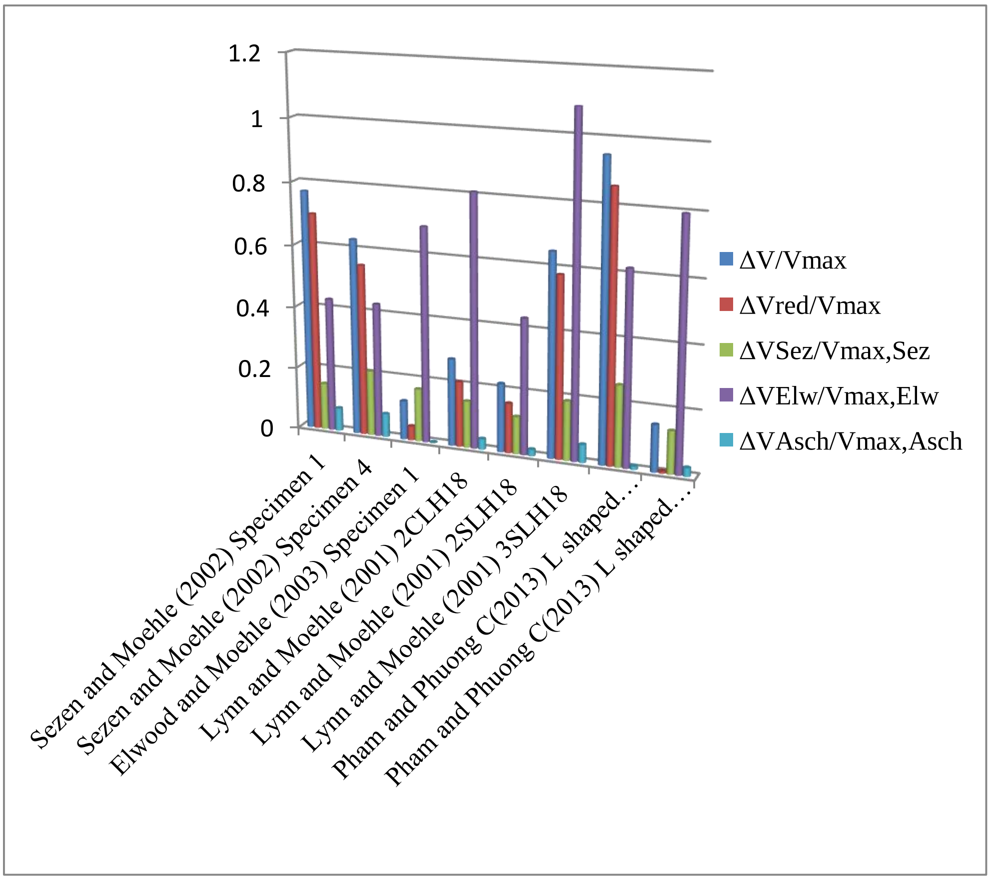

Figure 5 Distribution results for the calculations of ΔV,ΔV_{red},ΔV_{Sez},ΔV_{Elw} and ΔV_{Asch} for some of the specimens from the data base.

Specimens	$\frac{\Delta V}{V_{\max}}$	$\frac{\Delta V_{red}}{V_{\max}}$	$\frac{\Delta V_{Sez}}{V_{\max,Sez}}$	$\frac{\Delta V_{Elw}}{V_{\max,Elw}}$	$\frac{\Delta V_{Asch}}{V_{\max,Asch}}$
Sezen and Moehle (2002) Specimen 1	0.77	0.70	0.15	0.43	0.07
Sezen and Moehle (2002) Specimen 4	0.63	0.55	0.21	0.43	0.08
Elwood and Moehle (2003) Specimen 1	0.13	0.05	0.17	0.69	0.00
Lynn and Moehle (2001) Specimen 2CLH18	0.28	0.21	0.15	0.81	0.03
Lynn and Moehle (2001) Specimen 2SLH18	0.22	0.16	0.12	0.44	0.02
Lynn and Moehle (2001) Specimen 3SLH18	0.65	0.58	0.19	1.09	0.06
Pham and Phuong (2013) L shaped Columns- Specimen S1	0.95	0.86	0.26	0.62	0.01
Pham and Phuong (2013) L shaped Columns- Specimen S2	0.15	0.01	0.14	0.80	0.03

Table 2 Results from the calculations for μ=4, and $\frac{\Delta V}{V_{\max}}, \frac{\Delta V_{red}}{V_{\max}}, \frac{\Delta V_{Sez}}{V_{\max,Sez}}, \frac{\Delta V_{Elw}}{V_{\max,Elw}}, \frac{\Delta V_{Asch}}{V_{\max,Asch}}$.

Specimens	$\frac{\left(\frac{\Delta V_{red}}{V_{\max}}\right)}{\left(\frac{\Delta V}{V_{\max}}\right)}$	$\frac{\left(\frac{\Delta V_{Sez}}{V_{\max,Sez}}\right)}{\left(\frac{\Delta V}{V_{\max}}\right)}$	$\frac{\left(\frac{\Delta V_{Elw}}{V_{\max,Elw}}\right)}{\left(\frac{\Delta V}{V_{\max}}\right)}$	$\frac{\left(\frac{\Delta V_{Asch}}{V_{\max,Asch}}\right)}{\left(\frac{\Delta V}{V_{\max}}\right)}$
Sezen and Moehle (2002) Specimen 1	0.90	0.19	0.56	0.10
Sezen and Moehle (2002) Specimen 4	0.71	0.27	0.56	0.10
Elwood and Moehle (2003) Specimen 1	0.06	0.22	0.90	0.002
Lynn and Moehle (2001) Specimen 2CLH18	0.27	0.19	1.05	0.04
Lynn and Moehle (2001) Specimen 2SLH18	0.21	0.15	0.56	0.03
Lynn and Moehle (2001) Specimen 3SLH18	0.75	0.25	0.14	0.08
Pham and Phuong (2013) L shaped Columns- Specimen S1	1.12	0.34	0.80	0.01
Pham and Phuong (2013) L shaped Columns- Specimen S2	0.01	0.18	1.03	0.04

Table 3 Comparison of the proposed models results with the experimental results, for displacement ductility μ=4

In the following figures, the experimental results of the database specimens are plotted against the results of the models listed in Table 1.

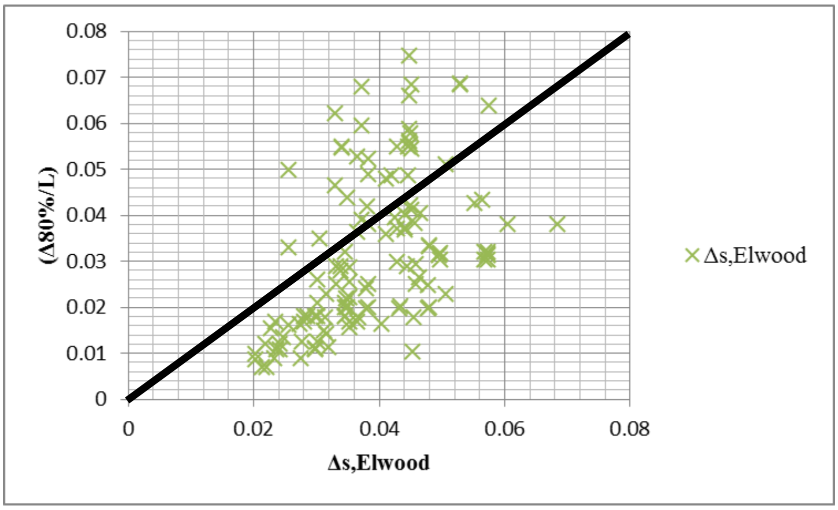

Figure 6 Comparisons between Elwood & Moehle (2003) proposed relationship for shear drift capacity of columns and the experimental values of the data base. The diagonal represents the equal value line.

Figure 7 compares experimental values of shear force with analytical peak lateral force values obtained after sectional analysis of the critical column cross section, using Response 2000 (2001) and considering second order effects; these values corresponding to the onset of shear failure (i.e., at Δ/L_s at a residual post peak strength of 80% of peak.)

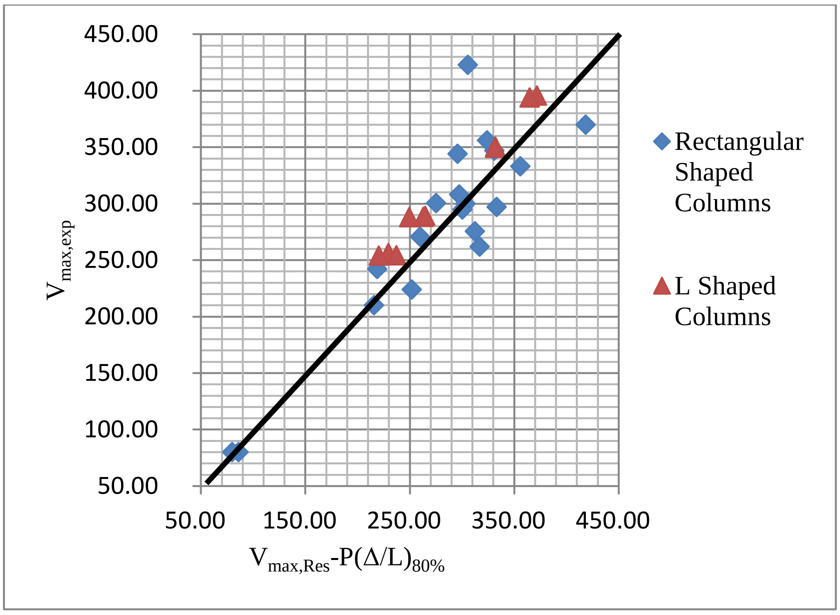

Figure 7 Correlation of $V_{max,exp}$ and $V_{max,Res}$- $P(\Delta/L)_{80\%}$

Results of a parametric investigation of the relationship between transverse reinforcement ratio, axial ratio, aspect ratio and experimental shear drift values are plotted in the following figures. Symbols used in Fig. 8 are color coded to represent the intensity of the axial load ratio (compressive) as follows:

◻ (blue)	$0 \leq v \leq 0.15$
◻ (red)	$0.15 \leq v \leq 0.3$
◻ (green)	$0.3 < v \leq 0.6$

Within each group, the rhomboid shape refers to low aspect ratio columns which are predisposed to shear failure; circles correspond to an aspect ratio between 2 and 4, whereas very slender members are plotted with triangles.

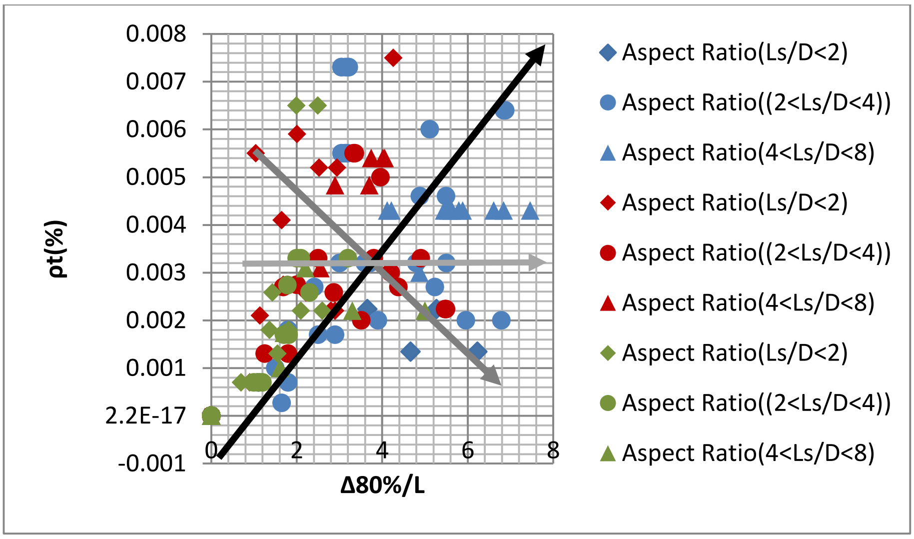

Figure 8 Influence of axial load ratio, transverse reinforcement ratio and aspect ratio, on drift ratio at shear failure.

From Figure 8 it is observed that several trends occur simultaneously: drift capacity at shear failure increases with the amount of transverse reinforcement, since better confinement and better shear reinforcement amounts postpone the occurrence of shear failure; green red and blue points are grouped sequentially in this order on the plot. Thus for the same amount of transverse reinforcement, specimens with higher axial load ratio correspond to lower values of lateral drift at shear failure. Higher drift values are possible as the axial load is reduced. Moreover for values of axial load in the range $0 \leq v \leq 0.15$ it may be seen that the drift capacity is proportional to transverse reinforcement ratio. Similar is the effect of the aspect ratio: higher aspect ratios lead to higher values of drift capacity at shear failure. This occurs whether as point of reference equal transverse reinforcement, or equal axial load ratio is considered.

Subsequently the value of drift at axial load failure as calculated by Eq. 9 is compared against its experimental counterpart in Figure 9; clearly the equation assesses the drift capacity at failure quire satisfactorily, however, the scatter is significant. It is possible that by accounting the other two important parameters, namely the aspect ratio and transverse reinforcement ratio the scatter may be reduced and correlation be improved.

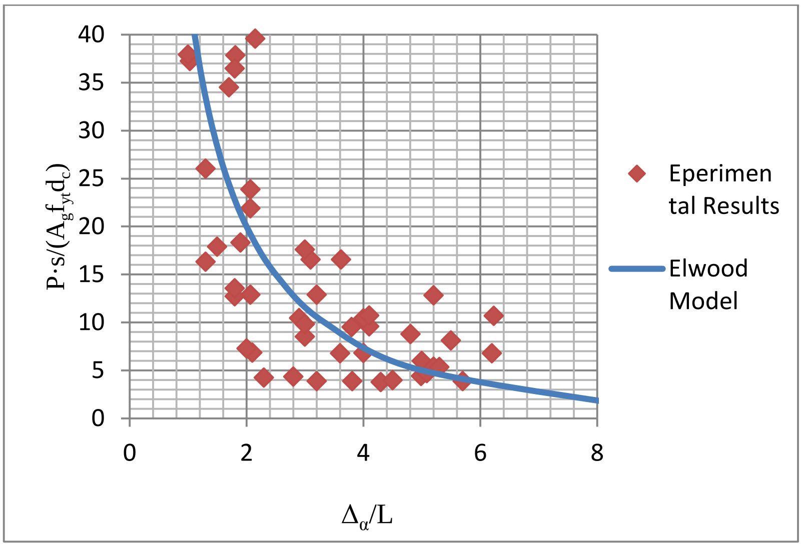

Figure 9 Comparison of experimental values of Δ_α with Elwood and Moehle (2003) proposed model.

6.0 CONCLUSIONS

- The current study aims to recapitulate the current knowledge concerning the estimation of the residual shear strength and pattern of strength degradation, taking into consideration the influence of axial load and the occurrence of second order effects during the lateral displacement history. Furthermore, drift capacities at the point associated with shear and axial load failures were also considered.
- Taking into account the contribution of axial load in estimating the remaining shear strength of a column with increasing displacement, it seems that a large fraction of the macroscopically observed lateral strength loss originally attributed to disintegration of the shear resistance mechanisms is really owing to the contribution of second order effects. This important response aspect accounts for a significant part of the lateral resistance of the column and therefore the coefficient of strength reduction with increasing ductility which has been introduced in assessment codes is found to overestimate the phenomena of strength degradation. Therefore, all the relevant assessment equations need to be reconsidered.
- Drift capacity at the onset of shear failure is defined at the point on the post peak branch associated with 80% residual member strength. After a parametric investigation, the results show that there is an agreement between the expressions by Elwood and Moehle (2003) and an independently assembled experimental database results in that the shear drift value increases almost proportionately with transverse reinforcement ratio, whereas it is inversely proportional to axial load ratio. Higher aspect ratio has the same effect; low shear drift values are observed in the case of shear critical columns.

6.0 REFERENCES

[1] Eurocode 8 (2005). Design of structures for earthquake resistance – Part.3: Assessment and retrofitting of buildings, European Committee for Standardization.

[2] Asadollah Esmaeily-Gh. and Yan Xiao, “Seismic Behavior of Bridge Columns Subjected to Various Loading Patterns”, *PEER Report No 2002/15*. University of California, Berkeley , December 2002.

[3] Lynn, A. C., “Seismic Evaluation of Existing Reinforced Concrete Building Columns,” *PhD dissertation*, Department of Civil and Environmental Engineering, University of California, Berkeley, Berkeley, Calif. 2001.

[4] Sezen, H., “Seismic Response and Modeling of Reinforced Concrete Building Columns,” *PhD dissertation*, Department of Civil and Environmental Engineering, University of California, Berkeley, 2002.

[5] Chasioti G.S., K.G.Megalooikonomou & S.J. Pantazopoulou ,” Shear Strength Assessment of Reinforced Concrete Columns”, *CD ROM Proceedings*, Thematic Conference on Computational Methods in Structural Dynamic and Earthquake Egineering (COM-DYN 2013), Kos Island, Greece 12-14 June 2013.

[6] Curtis J.Holub., “Interaction of Variable Axial Load and Shear Effects in RC Bridges”, *PhD dissertation*, Dep. Civil Engineering of University of Illionis at Urbana-Champaign, 2009.

[7] Sashi K.Kunnath, Ashraf El-Bahy & Andrew W.Taylor,W.C. Stone,” Cumulative Seismic Damage of Reinforced Concrete Bridge Piers”, *Report of Building and Fire Research Laboratory* NISTR 6075 ,NIST, Gaithersburg,MD 20899 October 1997.

[8] Kenneth J. Elwood & Jack P. Moehle, “Shake Table Tests and Analytical Studies on The Gravity Load Collapse of Reinforced Concrete Frames”, *PEER Report No 2003/01*, University of California, Berkeley, November 2003.

[9] Evan C. Bentz, Frank J. Vecchio, and Michael P. Collins, “Simplified Modified Compression Field Theory For Calculating Shear Strength of Reinforced Concrete Elements”, *ACI Structural J.* V103-No S65,July-August 2006.

[10] Cao Thanh Ngoc Tran & Bing Li ,”Ultimate Displaceent of Reinforced Concrete Columns with Light Transverse Reinforcement”, *J. Earthquake Engineering*, V. 17:2 No 282-300, 08 Jan 2013.

[11] Lisa Matchulat, “Mitigation of Collapse Risk In Vulnerable Concrete Buildings”, *M.Sc. Dissertation*, Department of Civil Engineering of Kansas University, 2008.

[12] Mark Aschheim & Jack P. Moehle, “Shear Strength and Deformability of RC Bridge Columns Subjected to Inelastic Cyclic Displacements", *Report No UCB/EERC-93/04*, March 1992.

[13] Pham, Thanh Phuong & Li, Binq, “Seismic Performance Assessment of L-Shaped Reinforced Concrete Columns”, *ACI Structural J.* No S-2013-225.R3, August 2013.

[14] ASCE/SEI 41 (2007). Seismic Rehabilitation of Existing Buildings, American Society of Civil Engineers.

[15] Response – 2000, Reinforced Concrete Sectional Analysis using the Modified Compression Field Theory, E. Bentz and P.Collins, Version 1.0.5, 2000.

[16] Pham, Thanh Phuong & Li, Binq, “Seismic Performance of Reinforced Concrete Columns With Plain Longitudinal Reinforcing Bars ”, *ACI Structural J.* No 111-S46, June2014.

[17] Yi-An Li, Yi-Tong Huang, and Shyh-Jiann Hwang, " Seismic Response of Rein-forced Concrete Short Columns Failed in Shear", *ACI Structural J.*, No 111-S80, August 2014.

[18] Y. Li, K.J. Elwood & S.-J. Hwang , " Assessment of ASCE/SEI 41 Concrete Column Provisions using Shaking Table Tests", ACI SP297-2, June 2014.

[19] M. Di Ludovico, G.M. Verderame, A. Prota, G. Manfredi, and E. Cosenza," Cyclic Behaviot Of Non-Conforming Full Scale RC Columns", J. of Structural Engineering, No. 10.1061/(ASCE)ST.1943-541X.0000891, June 2013.

[20] J.C.M. Ho and H.J. Pam, "Influence of Transverse Steel Configuration on Post-elastic Behaviour of High-strength Reinf. Concrete Columns", J. of HKIE TRANSACTIONS,Taylor & Francis, Apr 2013.

Appendix A

Specimens	B (mm)	D or h (mm)	L(mm)	fc'	a/D	ρl(%)	fyl(Mpa)	s(mm)	ρt(%)	fyt(Mpa)	P/Agfc'
Bechtoula,Kono,Arai and Watanade,2002,											
DIN 2002	250	250	625	37.60	2.5	0.02	461	40	0.01	485	0.30
Esaki ,1996											
H-2-1/3	200	200	400	23	2	0.03	363	40	0.01	363	0.33
H-2-1/5	200	200	400	23	2	0.03	363	50	0.01	364	0.20
HT-2-1/3	200	200	400	20	2	0.03	363	60	0.01	364	0.33
HT-2-1/5	200	200	400	20	2	0.03	363	75	0.01	364	0.20
Galeota et al 1996											
AB2	250	250	1,140	80	4.56	0.06	579	150	0.01	579	0.30
AB3	250	250	1,140	80	4.56	0.06	579	150	0.01	579	0.30
AB4	250	250	1,140	80	4.56	0.06	579	150	0.01	579	0.20
Nosho et al 1996											
AB2	279	279	2,134	40.6	7.64	0.01	407	229	0.001	351	0.34
Ohue et al. 1985											
2D16RS	200	200	400	32	2	0.02	369.00	50	0.005	316	0.14
4D13RS	200	299	400	30	2	0.03	370.00	50	0.005	316	0.15
Pujol 2002											
No.10-1-2.25N	152.4	304.8	686	36.5	2.25	0.02	453	57	0.01	411	0.08
No.10-1-2.25S	152.4	304.8	686	36.5	2.25	0.02	453	57	0.01	411	0.08
No.10-2-2.25N	152.4	304.8	686	34.9	2.25	0.02	453	57	0.01	411	0.08
No.10-2-2.25S	152.4	304.8	686	34.9	2.25	0.02	453	57	0.01	411	0.08
No.10-2-3N	152.4	304.8	686	33.7	2.25	0.02	453	76	0.01	411	0.09
No.10-2-3S	152.4	304.8	686	33.7	2.25	0.02	453	76	0.01	411	0.09
No.10-3-2.25N	152.4	304.8	686	27.4	2.25	0.02	453	57	0.01	411	0.10
No.10-3-2.25S	152.4	304.8	686	27.4	2.25	0.02	453	57	0.01	411	0.10
No.10-3-3N	152.4	304.8	686	29.9	2.25	0.02	453	76	0.01	411	0.10
No.10-3-3S	152.4	304.8	686	29.9	2.25	0.02	453	76	0.01	411	0.10
No.20-3-3N	152.4	304.8	686	36.4	2.25	0.02	453	76	0.01	411	0.16
No.20-3-3N	152.4	304.8	686	36.4	2.25	0.02	453	76	0.01	411	0.16
Ramirez and Jirsa , 1980											
00-U	305	305	458	34.5	1.5	0.02	374	65	0	455	-
Saatcioglu and Oscebe 1989											
U1	350	350	1,000	43.6	2.86	0.03	430	150	0.003	470	-
U2	350	350	1,000	30.2	2.86	0.03	453	150	0.003	470	0.16
U3	350	350	1,000	34.8	2.86	0.03	430	75	0.006	470	0.14
Soesianawati et al. 1986											
No.4	400	400	1,600	40	4	0.02	446	0.003	0.003	0.30	0.32
Takemura and Kawashima, 1997											

Test 1 (JSCE-4)	400	400	1,245	35.9	3.11	0.02	363	70	0.002	368	0.30
Test 2 (JSCE-4)	400	400	1,245	35.7	3.11	0.02	363	70	0.002	368	0.03
1997, Test 3 (JSCE-4)	400	400	1,245	34.3	3.11	0.02	363	70	0.002	368	0.03
1997, Test 4 (JSCE-4)	400	400	1,245	33.2	3.11	0.02	363	70	0.002	368	0.03
1997, Test 5 (JSCE-4)	400	400	1,245	36.8	3.11	0.02	363	70	0.002	368	0.03
Umehara and Jirsa 1982											
2CUS	230	410	455	42	1.11	0.03	441	89	0.01	414	0.27
Wehbe et al 1998											
A1	380	610	2,335	27.2	3.83	0.02	448	110	0.003	428	0.10
A2	380	610	2,335	27.2	3.83	0.02	448	110	0.003	428	0.24
Wight and Sozen 1973											
No.00.033(East)	152.4	304.8	876.0	32.0	2.88	0.02	496	127	0.003	345	-
No.00.033(West)	152.4	304.8	876.0	32.0	2.88	0.02	496	127	0.003	345	-
No.25.033(East)	152.4	304.8	876.0	33.6	2.88	0.02	496	127	0.003	345	0.07
No.25.033(West)	152.4	304.8	876.0	33.6	2.88	0.02	496	127	0.003	345	0.07
No.40.048(East)	152.4	304.8	876.0	26.1	2.88	0.02	496	89	0.005	345	0.15
No.40.048(West)	152.4	304.8	876.0	26.1	2.88	0.02	496	89	0.005	345	0.15
No.40.067(East)	152.4	304.8	876.0	33.4	2.88	0.02	496	64	0.01	345	0.11
No.40.067(West)	152.4	304.8	876.0	33.4	2.88	0.02	496	64	0.01	345	0.11
Xiao and Martyrossyan 1998											
HC4-8L16-T6-0.1P	254	254	508	86	2	0.02	510	51	0.01	449	0.10
HC4-8L16-T6-0.1P	254	254	508	86	2	0.02	510	51	0.01	449	0.19
Matchulat (2008)											
Specimen 1	457	457	2946.4	20.68	3.74	0.03	441.26	460	0.00	372.32	0.50
Specimen 2	457	457	2946.4	23.42	3.74	0.03	441.26	460	0.00	372.32	0.35
Elwood and Moehle (2003)											
Specimen 1	230	230	1470	25.55	3.69	0.03	689.48	150	0.02	689.48	0.10
Specimen 2	230	230	1470	23.92	3.69	0.03	689.48	150	0.02	689.48	0.24
Sezen and Moehle (2002)											
Specimen 1	457	457	2946.4	21.10	3.85	0.03	434.37	305	0.002	476	0.15
Specimen 2	457	457	2946.4	21.10	3.85	0.03	434.37	305	0.002	476	0.60
Specimen 4	457	457	2946.4	21.79	3.85	0.03	434.37	305	0.002	476	0.15
Lynn and Moehle (2001)											
Specimen 3CLH18	457	457	2946	25.58	3.66	0.03	330.95	460	0.001	400	0.12
Specimen 2CLH18	457	457	2946	33.09	3.63	0.02	330.95	460	0.001	400	0.12
Specimen 3SLH18	457	457	2946	25.58	3.66	0.03	330.95	460	0.001	400	0.12
Specimen 2SLH18	457	457	2946	33.09	3.63	0.02	330.95	460	0.001	400	0.12
Specimen 2CMH18	457	457	2946	25.51	3.63	0.02	330.95	460	0.001	400	0.35
Specimen 3CMH18	457	457	2946	27.58	3.66	0.03	330.95	460	0.001	400	0.35
Specimen 3CMD12	457	457	2946	27.58	3.66	0.03	330.95	460	0.002	400	0.35
Specimen 3SMD12	457	457	2946.4	25.51	3.63	0.03	330.95	460	0.002	400	0.35
Phuong and Li (2012)											

S-2.4-0.3	350	350	1700	49.3	2.77	0.03	409	130	0.001	393	0.30
SC-2.4-0.2	350	350	1700	22.6	2.75	0.02	409	130	0.001	393	0.20
SC-2.4-0.5	350	350	1700	24.2	2.75	0.02	409	130	0.001	393	0.50
SC-1.7-0.2	350	350	1200	27.5	1.94	0.02	409	130	0.001	393	0.20
SC-1.7-0.5	350	350	1200	26.4	1.94	0.02	409	130	0.001	393	0.50
M.D. Ludovico et al.(2013)											
S300D-C	300	300	1500	22.71	2.93	0.01	520	150	0.002	520	0.20
R300D-C	500	300	1500	22.71	1.64	0.01	520	150	0.001	520	0.10
R500D-C	300	500	900	22.71	1.76	0.01	520	150	0.002	520	0.10
S300P-C(plain re-bars)	300	300	1500	22.71	2.93	0.01	330	150	0.002	330	0.20
R300P-C(plain re-bars)	500	300	1500	22.71	1.64	0.01	330	150	0.001	330	0.10
R500P-C(plain re-bars)	300	500	900	22.71	1.76	0.01	330	150	0.002	330	0.10
Henkhaus, Pujol and Ramirez (2013)											
B1	457	457	1473	20.0	1.90	0.02	455	457	0.001	490	0.37
B2	457	457	1473	19.3	1.90	0.02	455	457	0.001	455	0.38
B3	457	457	1473	22.1	1.90	0.02	455	457	0.001	490	0.21
B4	457	457	1473	24.1	1.90	0.03	441	457	0.001	490	0.43
B5	457	457	746.5	23.4	1.90	0.03	441	457	0.001	490	0.46
B6	457	457	2947	27.6	3.70	0.03	490	305	0.002	469	0.11
B7	457	457	2947	28.3	3.70	0.03	490	305	0.002	469	0.11
B8	457	457	2947	29.0	3.70	0.03	490	305	0.001	490	0.11
Wood's (2010)											
Specimen 3	457	457	2946	17.31	3.72	0.03	441.26	457	0.0007	372.32	0.50
Specimen 4	457	457	2946	18.62	3.72	0.03	448.16	305	0.0003	372.32	0.15
Thanh Phuong Pham and Bing Li 2014 (smooth bars)											
SP1-1.7-0.2	350	350	1200	29.8	1.7	0.02	320	125	0.003	500	0.20
SP2-1.7-0.35	350	350	1200	29.2	1.7	0.02	320	125	0.003	500	0.35
SP3-2.4-0.2	350	350	1700	30.6	2.4	0.02	320	125	0.003	500	0.20
SP4-2.4-0.35	350	350	1700	28.7	2.4	0.02	320	125	0.003	500	0.35
SR1-1.7-0.35	250	490	1700	23.3	1.7	0.02	320	125	0.002	500	0.35
SR2-1.7-0.5	250	490	1700	22.5	1.7	0.02	320	125	0.002	500	0.50
J C M HO and H J PAM (2013)											
8S-60-06-61-S	325	325	1515	56.6	5.00	0.06	525	100	0.002	378	0.54
8S-60-06-61-C	325	325	1515	60.4	5.03	0.06	525	210	0.002	357	0.53
)8S-100-03-24-S	325	325	1515	95.1	4.93	0.02	522	100	0.003	357	0.28
8S-100-03-24-C	325	325	1515	109.5	4.93	0.02	522	150	0.003	357	0.31
NEW-60-06-61-S	325	325	1515	57.1	5.26	0.06	525	100	0.010	531	0.53
NEW-60-06-61-C	325	325	1515	62.4	5.26	0.06	525	210	0.002	531	0.53
NEW-l00-03-24-S	325	325	1515	96.5	5.26	0.02	522	70	0.009	531	0.28
NEW-l00-03-24-C	325	325	1515	108.4	5.26	0.02	522	90	0.012	531	0.30
8S'-100-02-15-900	325	325	1515	111.1	5.19	0.02	572	150	0.005	367	0.20
8S'-100-02-15-45°	325	325	1515	109.4	5.19	0.02	572	150	0.005	367	0.21

Specimens	D or h (mm)	L(mm)	fc'	a/D	ρl(%)	fyl(Mpa)	s(mm)	ρt(%)	fyt(Mpa)	P/Ag-fc'
Kunnath et al.1997										
A2	304.8	1372	29.041	5.6232	0.02	448.2	190.5	0.0043	430.491	0.0944
A3	304.8	1372	29.041	5.622	0.02	448.2	190.5	0.0043	430.491	0.0944

A4	304.8	1372	35.517	5.622	0.02	448.2	190.5	0.0043	430.491	0.0856
A5	304.8	1372	35.52	5.622	0.02	448.2	190.5	0.0043	430.491	0.0856
A6	304.8	1372	35.52	5.622	0.02	448.2	190.5	0.0043	430.491	0.0856
A7	304.8	1372	32.816	5.6232	0.02	448.2	190.5	0.0043	430.491	0.0926
A8	304.8	1372	32.82	5.6232	0.02	448.2	190.5	0.0043	430.491	0.0926
A9	304.8	1372	32.516	5.6232	0.02	448.2	190.5	0.0043	430.491	0.0935
A10	304.8	1372	27.0135	5.6232	0.02	448.2	190.5	0.0043	430.491	0.101
A11	304.8	1372	27.01	5.6232	0.02	448.2	190.5	0.0043	430.491	0.101
A12	304.8	1372	27.01	5.6232	0.02	448.2	190.5	0.0043	430.491	0.101
Arakawa et al. 1987										
UNIT1	275.08	600	28.81	1.36	0.04	366.2	100	0.002	368.18	0
UNIT2	275.08	600	29.31	1.36	0.04	366.2	50	0.004	368.18	0
UNIT 4	275.08	600	29.81	1.36	0.04	366.2	100	0.002	368.18	0.12
UNIT 6	275.08	600	28.61	1.36	0.04	366.2	50	0.004	368.18	0.12
UNIT 8	275.08	600	31.41	1.36	0.04	366.2	35	0.005	368.18	0.12
UNIT 9	275.08	600	30.51	1.36	0.05	366.2	50	0.004	368.18	0.12
UNIT 12	275.08	600	27.81	1.36	0.04	366.2	100	0.002	368.18	0.26
UNIT 13	275.08	600	30.51	1.36	0.04	366.2	50	0.004	368.18	0.24
UNIT 14	275.08	600	31.31	1.36	0.04	366.2	35	0.005	368.18	0.23
UNIT 17	275.08	600	31.31	1.36	0.04	363.2	75	0.003	381.19	0.12
UNIT 19	275.08	900	31.31	2.04	0.04	363.2	75	0.003	381.19	0.12
UNIT 22	275.08	900	20.51	2.04	0.04	363.2	75	0.003	381.19	0.18
UNIT 24	275.08	600	31.11	1.36	0.04	363.2	75	0.003	381.19	0.23
UNIT 25	275.08	900	29.71	2.04	0.04	363.2	75	0.003	381.19	0.24
UNIT 27	275.08	900	18.90	2.04	0.04	363.2	75	0.003	381.19	0.38
UNIT 28	275.08	900	41.32	2.04	0.04	363.2	75	0.003	381.19	0.18

Pham and Phuong 2013												
Speci-mens	b(mm)	h(mm)	h'(mm)	Ls(mm)	fc' (Mpa)	a/D	ρl(%)	fyl(Mpa)	s(mm)	ρt(%)	fyt(Mpa)	P/Ag-fc'
S1	170	430	414	1700	29.8	2.05	0.02	465	100	0.003	467	0.2
S2	170	430	414	1700	29.2	2.05	0.02	465	100	0.003	467	0.35
S3	170	430	414	1700	29.2	2.05	0.02	465	100	0.003	467	0.2
S4	170	430	414	1700	29.4	2.05	0.02	465	100	0.003	467	0.35
S5	170	430	414	1700	29.1	2.05	0.02	465	100	0.003	467	0.2
S6	170	430	414	1700	29.1	2.05	0.02	465	100	0.003	467	0.35
S13	170	430	414	1200	27	1.45	0.02	465	150	0.002	467	0.2
S14	170	430	414	1200	27.4	1.45	0.02	465	150	0.002	467	0.35
S15	170	430	414	1200	26.8	1.45	0.02	465	150	0.002	467	0.2
S16	170	430	414	1200	27.2	1.45	0.02	465	150	0.002	467	0.35

Table 4 : Data Base

Appendix B

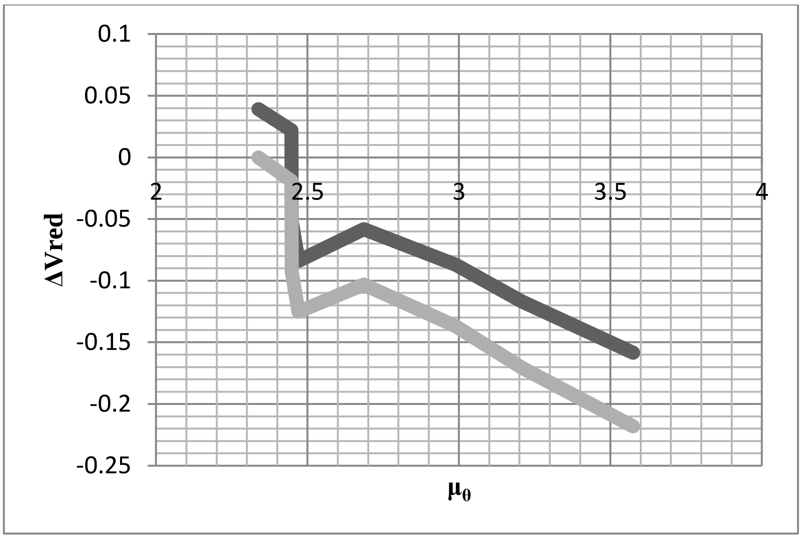

Figure 10 Difference between the experimental and the corrected shear strength degradation with increasing μ_θ

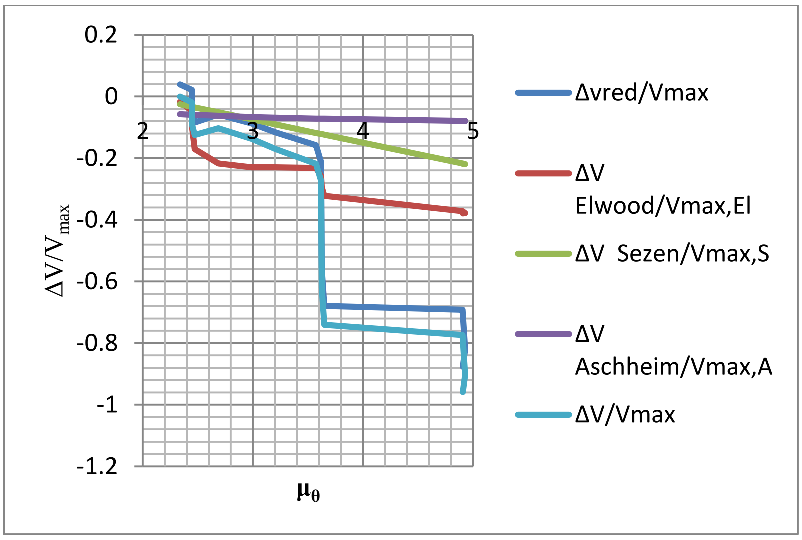

Figure 11 Comparisons between ΔVred ,ΔV from the experimental data base with ΔV according with the models by Sezen and Moehle (2002), Aschheim and Moehle (1992) and Elwood and Moehle (2003) .